

Mercury's solar wind interaction as characterized by magnetospheric plasma mantle observations with MESSENGER

Jamie M. Jasinski ¹, James A. Slavin ¹, Jim M. Raines ¹ and Gina. A. DiBraccio ²

1. Dept. of Climate and Space Sciences and Engineering, University of Michigan, Ann Arbor, MI, USA.
2. NASA Goddard Space Flight Center, Greenbelt, MD, USA.

Contents of this file

Introduction
Figures S1.
Table S1.

Introduction

Included in the online supporting material is the observation of the plasma mantle on the 28th of September 2011 as described in Section 3.4.1 of the main paper. This figure shows the largest difference between the selection of the magnetopause by our algorithm and the field rotation of the magnetopause selected visually.

Also included is a list of plasma mantle crossings.

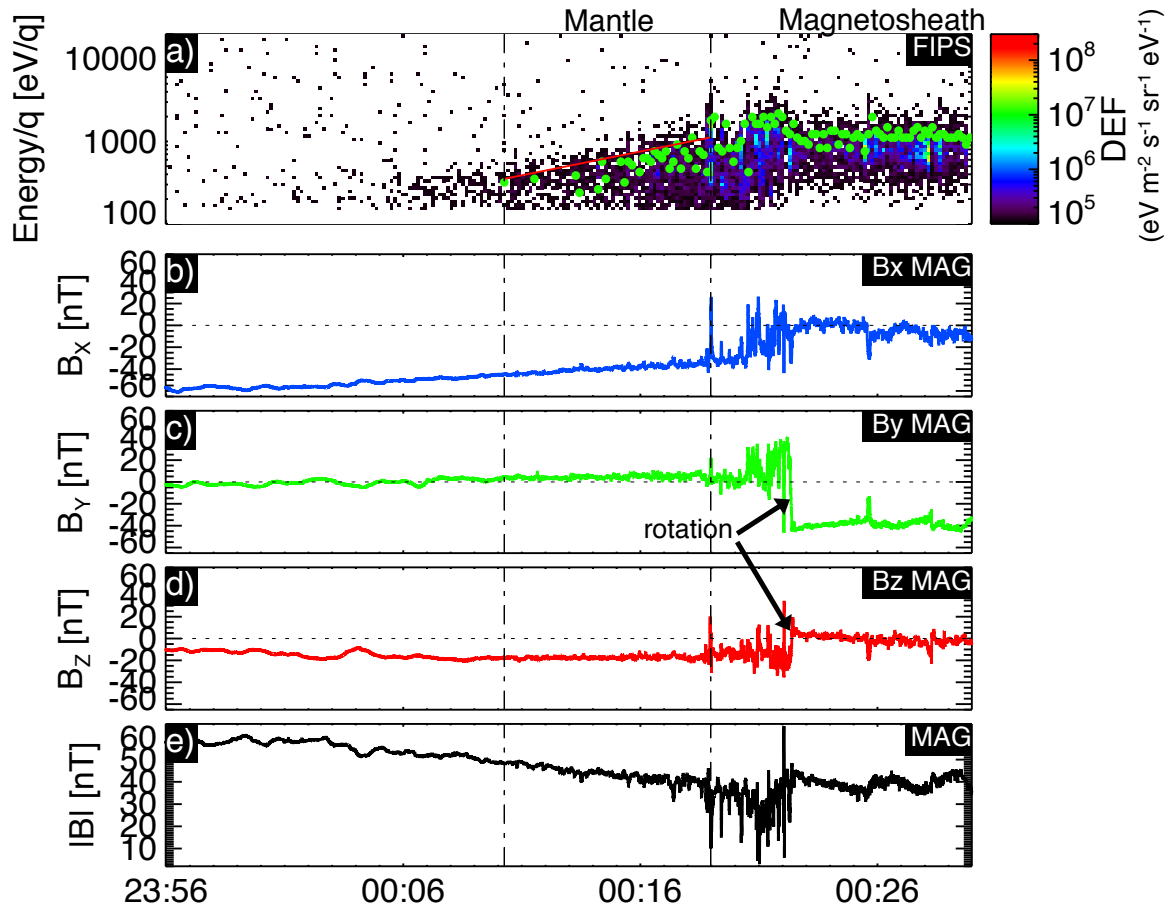


Figure S1. MESSENGER observation of the plasma mantle on the 28th of September 2011. From top to bottom: a) proton differential energy flux (DEF) measured by FIPS with the green dot showing the highest energy bin with a signal-to-noise ratio ≥ 2 , and the red line highlighting the dispersion ; b-d) the three components of the magnetic field in MSO coordinates measured by MAG, and e) magnetic field magnitude also measured by MAG. The dashed vertical lines show the selection of the mantle. The field rotation labeled 'rotation' can be seen approximately ~3 minutes after the second dashed line.

Table S1. Times of the plasma mantle crossings (start and stop) by the MESSENGER spacecraft, as selected by our algorithm described in the main article. 'DOY' stands for day of year.

Day	Month	Year	Start			Stop			DOY
			hour	minute	second	hour	minute	second	
12	4	2011	17	30	33.7	17	33	24.7	102
13	4	2011	5	28	24.7	5	30	8.7	103
13	4	2011	17	35	17.7	17	36	33.7	103
15	4	2011	17	48	31.7	17	51	50.7	105
16	4	2011	5	36	42.7	5	43	40.7	106
16	4	2011	17	47	5.7	17	50	44.7	106
22	6	2011	11	31	30.4	11	42	16.4	173
22	6	2011	23	13	55.4	23	22	38.4	173
25	6	2011	22	24	59.4	22	33	14.4	176
26	6	2011	22	1	29.4	22	7	59.4	177
2	7	2011	7	48	44.4	7	55	5.4	183
3	7	2011	19	18	44.4	19	22	32.4	184
28	9	2011	0	10	21.3	0	18	55.3	271
29	9	2011	11	34	34.3	11	39	9.3	272
5	10	2011	20	19	57.3	20	27	14.3	278
6	10	2011	8	13	4.3	8	22	43.3	279
10	10	2011	17	54	24.3	18	3	45.3	283
19	11	2011	8	26	42.4	8	43	10.4	323
19	11	2011	20	26	0.4	20	28	51.4	323
23	11	2011	8	41	18.4	8	54	27.4	327
22	12	2011	4	1	19.8	4	7	59.8	356
30	12	2011	0	35	1.8	0	43	25.8	364
31	12	2011	23	37	51.8	23	48	37.8	365
1	1	2012	23	10	1.8	23	23	29.8	1
2	1	2012	22	47	37.8	22	53	9.8	2
16	3	2012	21	28	23.7	21	35	6.7	76
17	3	2012	9	0	48.7	9	9	28.7	77
20	3	2012	6	45	2.7	6	50	20.7	80
12	5	2012	5	52	54.8	6	0	41.8	133
20	6	2012	16	22	3.9	16	28	15.9	172
21	6	2012	0	26	19.9	0	39	36.9	173
30	6	2012	8	22	19.9	8	26	12.9	182
8	8	2012	13	52	24.0	14	10	18.0	221
12	9	2012	8	48	2.0	8	53	11.0	256
16	9	2012	9	4	36.0	9	7	5.0	260
10	11	2012	6	35	3.1	6	47	49.1	315
10	11	2012	14	30	28.1	14	45	32.1	315

7	12	2012	9	7	11.2	9	10	55.2	342
9	12	2012	17	1	40.2	17	11	36.2	344
10	12	2012	9	16	36.2	9	23	53.2	345
16	12	2012	16	55	26.2	17	11	14.2	351
17	12	2012	8	54	3.2	9	2	56.2	352
3	2	2013	22	41	8.2	22	50	0.2	34
8	3	2013	9	36	46.3	9	39	47.3	67
13	3	2013	17	18	5.3	17	29	6.3	72
14	3	2013	9	42	22.3	9	46	38.3	73
2	5	2013	7	11	57.4	7	26	8.4	122
1	6	2013	17	57	50.4	18	0	30.4	152
4	6	2013	2	4	59.4	2	8	10.4	155
8	6	2013	10	10	12.4	10	13	2.4	159
22	7	2013	15	27	50.5	15	35	7.5	203
23	7	2013	7	33	57.5	7	36	37.5	204
24	7	2013	15	39	35.5	15	52	11.5	205
17	10	2013	16	11	24.6	16	17	59.6	290
18	10	2013	8	11	15.6	8	20	29.6	291
29	10	2013	16	20	36.6	16	38	0.6	302
18	1	2014	0	46	15.8	0	54	15.8	18
18	1	2014	8	43	1.8	8	58	6.8	18
22	1	2014	8	48	21.8	8	53	50.8	22
27	1	2014	9	10	53.8	9	23	41.8	27
16	2	2014	3	6	13.8	3	49	11.8	47
10	4	2014	9	27	23.9	9	46	12.9	100
18	4	2014	9	22	10.9	9	25	54.9	108
19	4	2014	1	21	59.9	1	26	47.9	109
23	4	2014	17	33	9.9	17	37	46.9	113
24	5	2014	12	25	3.0	12	48	30.0	144
27	5	2014	19	58	12.0	20	24	50.0	147
2	7	2014	19	30	43.3	19	36	3.3	183
5	7	2014	3	56	9.3	4	0	25.3	186
8	7	2014	4	8	55.3	4	10	21.3	189
9	7	2014	12	17	31.3	12	18	24.3	190
16	8	2014	2	49	48.4	2	51	34.4	228
25	8	2014	3	18	16.4	3	49	52.4	237
27	9	2014	6	59	11.7	7	12	9.7	270
29	9	2014	15	32	18.7	15	39	56.7	272
29	9	2014	23	38	29.7	23	40	36.7	272
30	9	2014	7	44	57.7	7	49	24.7	273
6	10	2014	9	23	54.7	9	31	43.7	279
9	10	2014	2	1	24.7	2	5	39.7	282
25	12	2014	4	31	51.2	4	43	35.2	359

30	12	2014	15	56	15.2	16	2	17.2	364
31	12	2014	0	8	1.2	0	9	57.2	365
7	1	2015	12	48	0.2	12	54	23.2	7
8	1	2015	5	15	17.2	5	17	46.2	8
10	1	2015	6	23	23.2	6	37	35.2	10
12	1	2015	16	8	51.2	16	15	25.2	12
23	3	2015	6	24	45.7	6	32	44.7	82
31	3	2015	13	26	16.7	13	33	1.7	90
3	4	2015	7	48	57.9	7	50	1.9	93
5	4	2015	1	23	26.0	1	28	25.0	95
6	4	2015	10	40	49.4	10	46	9.4	96
7	4	2015	11	40	47.8	11	44	53.8	97
8	4	2015	4	21	30.3	4	28	15.3	98
10	4	2015	23	3	22.9	23	9	56.9	100